



---

*Research article*

## **A lattice model for active–passive pedestrian dynamics: a quest for drafting effects**

**Emilio N. M. Cirillo<sup>1</sup>, Matteo Colangeli<sup>2</sup>, Adrian Muntean<sup>3</sup> and T. K. Thoa Thieu<sup>4,\*</sup>**

<sup>1</sup> Department of Basic and Applied Sciences for Engineering, Sapienza University, Roma

<sup>2</sup> Department of Information Engineering, Computer Science and Mathematics, University of L'Aquila, Italy

<sup>3</sup> Department of Mathematics and Computer Science, Karlstad University, Sweden

<sup>4</sup> Department of Mathematics, Gran Sasso Science Institute, L'Aquila, Italy

\* **Correspondence:** Email: [thikimthoa.thieu@gssi.it](mailto:thikimthoa.thieu@gssi.it).

**Abstract:** We study the pedestrian escape from an obscure room using a lattice gas model with two species of particles. One species, called passive, performs a symmetric random walk on the lattice, whereas the second species, called active, is subject to a drift guiding the particles towards the exit. The drift mimics the awareness of some pedestrians of the geometry of the room and of the location of the exit. We provide numerical evidence that, in spite of the hard core interaction between particles – namely, there can be at most one particle of any species per site – adding a fraction of active particles in the system enhances the evacuation rate of all particles from the room. A similar effect is also observed when looking at the outgoing particle flux, when the system is in contact with an external particle reservoir that induces the onset of a steady state. We interpret this phenomenon as a discrete space counterpart of the drafting effect typically observed in a continuum set-up as the aerodynamic drag experienced by pelotons of competing cyclists.

**Keywords:** pedestrian dynamics; evacuation; obscure room; simple exclusion dynamics; particle currents; drafting

---

### **1. Introduction**

This work is part of a larger recent research initiative oriented towards investigating the evacuation behavior of crowds of pedestrians where the geometry in which the dynamics takes place is partly unknown and possibly also with limited visibility. Such scenarios are encountered for instance when catastrophic situations occur in urban environments (e.g., in large office spaces), in tunnels, within underground spaces and/or in forests in fire. We refer the reader, for instance, to [1–5] and references

cited therein, as well as to our previous results; see e.g. [6]. Experimental information in this context is provided, for instance, in [7] and [8] (also in connection with what is usually referred to as "faster-is-slower" effect). In the current framework, our hypothesis is that the crowd under consideration is always heterogeneous in the sense that some part of the population is well informed about the details of the geometry of the location and corresponding exits as well as of the optimal escape routes and consequently adapts its motion strategy, while the rest of the population has a passive attitude and move without following a precise strategy. This is exactly the standing assumption we have investigated in [9, 10] for a dynamics in smoke scenario.

It turns out that in situations where the information can only difficultly be transmitted from pedestrian to pedestrian (like when large crowds are present and/or if the geometry of the evacuation is largely unknown or invisible and/or groups are not able to act rationally), the use of leaders to guide crowds towards the exits might not always be possible, or it works inefficiently. In such cases, leadership is not essential to speed up evacuation\*. So, what can then be still done to improve evacuations for such unfavorable conditions, i.e. to decrease the evacuation time of the overall crowd? One of the main points we want to make here is the following: Even if information cannot be transmitted within the crowd, simply having a suitable fraction of informed pedestrians speeds up the overall evacuation time.

We study the typical time needed by a heterogeneous crowd of pedestrians to escape a dark room. The heterogeneity of the crowd is incorporated in the fact that we consider two pedestrian species, the *active* and the *passive* one, i.e., those who know the location of the exit and those who do not. Using a lattice-type model, we show that the presence of pedestrians aware of the location of the exit helps the unaware companions to find the exit of the room even in absence of any information exchange among them. This effect will be called *drafting* and it has a twofold interpretation: i) active particles, quickly moving towards the exit, will leave a wake of empty sites in which the unaware particles can jump in, so that they are guided to the exit; ii) active pedestrians, in their rational motion towards the exit, push their passive companions to the exit as well. People belonging to the same group do not necessarily have to move together or coherently, for they only share the same dynamical rules. In other words, the motion of one pedestrian is not directly affected by the motion of the pedestrians belonging to the same group. The sole interaction we consider here is the hard-core repulsion between any pair of pedestrians, regardless of their group. In this sense the situation we have in mind is different from the one considered in some experiments, where people in the same social group move coherently and not independently [7].

We refer the reader to for instance to [11–13] for some level of details on crowd dynamics modelling and to [14–16] for relevant works regarding the handling of the presence of the obstacles and the way they affect the pedestrian motion. Mind also that similar situations appear frequently also in soft matter physics cf. e.g. [18].

---

\*This is contrary to situations like those described on [17], where leadership is an efficient crowd management mechanism. Yet, often in pedestrian crowds there are no obvious leaders, such as those present, for instance, in political demonstrations. There is contrary evidence concerning the efficiency of the leadership in managing crowds. For instance, sometimes artists (who could be seen as leaders of crowds) have wrongly been accused of working against safety personnel or police. A famous example is that of the band Pearl Jam at the Roskilde Festival in 2001. A number of people died and responsibility was placed on the band and their actions. The inquiry that came later then altered this view. See some information on this matter can be found via <https://uproxx.com/music/pearl-jam-roskilde/>. Another example dates back to the 1989 Hillsborough Disaster. Using Hillsborough literature, police accused the crowds in the wake of the tragic event but, almost 30 years later, all accusations were dropped and blame was heavily placed on police and organisation. This article seems to cover it: [https://www.tandfonline.com/doi/full/10.1080/1466097042000235209?casa\\_token=07xM8m5HQScAAAAA:AU8DN18LPnuSv5a01w0iw3WXEXA2AHDE95M7szy6Wakzoq14v0c2Niv44wQK5WC1eDg\\_qYbNFJPLLA](https://www.tandfonline.com/doi/full/10.1080/1466097042000235209?casa_token=07xM8m5HQScAAAAA:AU8DN18LPnuSv5a01w0iw3WXEXA2AHDE95M7szy6Wakzoq14v0c2Niv44wQK5WC1eDg_qYbNFJPLLA).

The remainder of the paper is organized as follows. In Section 2 we define the model. Section 3 is devoted to the study of the evacuation time. In Section 4 a slightly modified version of the model is considered, so that a not trivial stationary state is reached. For such a model the stationary exit flux is thus studied. In Section 5, we summarize our conclusions and give a glimpse of possible further research.

## 2. The model

The *room* is the square lattice  $\Lambda = \{1, \dots, L\} \times \{1, \dots, L\} \subset \mathbb{Z}^2$  of side length  $L$ , with  $L$  an odd positive integer number, see Figure 1. An element  $x = (x_1, x_2)$  of the room  $\Lambda$  is called *site* or *cell*. Two sites  $x, y \in \Lambda$  are said *nearest neighbor* if and only if  $|x - y| = 1$ . We conventionally call *horizontal* the first coordinate axis and *vertical* the second one. The words *left*, *right*, *up*, *down*, *top*, *bottom*, *above*, *below*, *row*, and *column* will be used accordingly. We call *exit* a set of  $w_{\text{ex}}$  pairwise adjacent sites, with  $w_{\text{ex}}$  an odd positive integer smaller than  $L$ , of the top row of the room  $\Lambda$  symmetric with respect to its median column. In other words, the exit is a centered slice of the top row of the room mimicking the presence of an exit door. The number  $w_{\text{ex}}$  will be called *width* of the exit. Inside the top part of the room we define a rectangular interaction zone, namely, the *visibility region*  $V$ , made of the first  $L_v$  top rows of  $\Lambda$ , with the positive integer  $L_v \leq L$  called *depth* of the visibility region. By writing  $L_v = 0$ , we refer to the case in which no visibility region is considered.

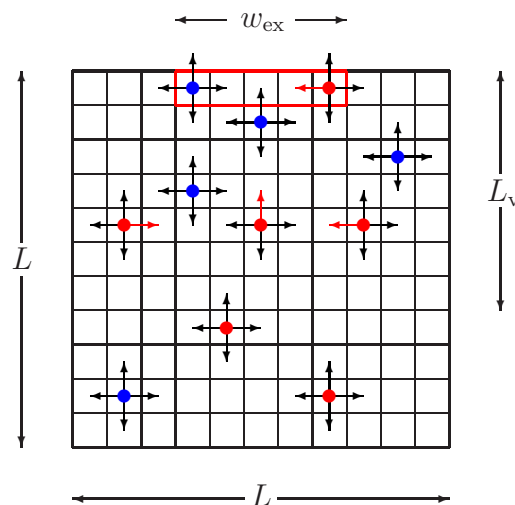


**Figure 1.** Schematic representation of our lattice model. Blue and red disks denote passive and active particles, respectively. The rectangle of sites delimited by the red contour denotes the exit. Black and red arrows (color online) denote transitions performed with rates 1 and  $1 + \varepsilon$ , respectively.

We consider two different species of particles, i.e., *active* and *passive*, moving inside  $\Lambda$  (we shall sometimes use in the notation the symbols  $A$  and  $P$  to respectively refer to them). Note that the sites of the external boundary of the room, that is to say the sites  $x \in \mathbb{Z}^2 \setminus \Lambda$  such that there exists  $y \in \Lambda$  nearest neighbor of  $x$ , cannot be accessed by the particles. The state of the system will be a *configuration*  $\eta \in \Omega = \{-1, 0, 1\}^\Lambda$  and we shall say that the site  $x$  is *empty* if  $\eta_x = 0$ , *occupied by an active particle*

if  $\eta_x = 1$ , and *occupied by a passive particle* if  $\eta_x = -1$ . The number of active (respectively, passive) particles in the configuration  $\eta$  is given by  $n_A(\eta) = \sum_{x \in \Lambda} \delta_{1, \eta_x}$  (resp.  $n_P(\eta) = \sum_{x \in \Lambda} \delta_{-1, \eta_x}$ ), where  $\delta_{\cdot, \cdot}$  is Kronecker's symbol. Their sum is the total number of particles in the configuration  $\eta$ .

The dynamics in the room is modeled via a simple exclusion random walk with the two species of particles undergoing two different microscopic dynamics: the passive particles perform a symmetric simple exclusion dynamics on the whole lattice, while the active particles, on the other hand, perform a symmetric simple exclusion walk outside the visibility region, whereas inside such a region they experience a drift pushing them towards the exit. In other words, the whole room is obscure for the passive particles, while, for the active ones, only the region outside the visibility region is obscure.

What concerns this precise setup, the dynamics is incorporated in the continuous time Markov chain  $\eta(t)$  on  $\Omega$  with rates  $c(\eta, \eta')$  defined as follows: Let  $\varepsilon \geq 0$  be the *drift*; for any pair  $x = (x_1, x_2), y = (y_1, y_2)$  of nearest neighbor sites in  $\Lambda$  we set  $\varepsilon(x, y) = 0$ , excepting the following cases in which we set  $\varepsilon(x, y) = \varepsilon$ :

- $x, y \in V$  and  $y_2 = x_2 + 1$ , namely,  $x$  and  $y$  belong to the visibility region and  $x$  is below  $y$ ;
- $x, y \in V$  and  $y_1 = x_1 + 1 < (L + 1)/2$ , namely,  $x$  and  $y$  belong to the left part of the visibility region and  $x$  is to the left with respect to  $y$ ;
- $x, y \in V$  and  $y_1 = x_1 - 1 > (L + 1)/2$ , namely,  $x$  and  $y$  belong to the right part of the visibility region and  $x$  is to the right with respect to  $y$ .

Next, we let the rate  $c(\eta, \eta')$  be equal

- to 1 if  $\eta'$  can be obtained by  $\eta$  by replacing with 0 a  $-1$  or a  $1$  at the exit (particles leave the room);
- to 1 if  $\eta'$  can be obtained by  $\eta$  by exchanging a  $-1$  with a  $0$  between two neighboring sites of  $\Lambda$  (motion of passive particles inside  $\Lambda$ );
- to  $1 + \varepsilon(x, y)$  if  $\eta'$  can be obtained by  $\eta$  by exchanging a  $+1$  at site  $x$  with a  $0$  at site  $y$ , with  $x$  and  $y$  nearest neighbor sites of  $\Lambda$  (motion of active particles inside  $\Lambda$ );
- to 0 in all the other cases.

The *infinitesimal generator*  $\mathcal{L}$  acts on continuous bounded functions  $f : \Omega \rightarrow \mathbb{R}$  as

$$\mathcal{L}(\eta) = \sum_{\eta' \in \Omega} c(\eta, \eta') [f(\eta') - f(\eta)]. \quad (2.1)$$

The probability measure induced by the Markov chain started at  $\eta$  is denoted by  $P_\eta$  and the related expectation is denoted by  $E_\eta$ . We refer to [19, 20] where similarly–in–spirit models are described mathematically in a rigorous fashion.

The initial number of active (respectively, passive) particles is denoted by  $N_A = n_A(\eta_x(0))$  (respectively,  $N_P = n_P(\eta_x(0))$ ). We also let  $N = N_A + N_P$  be the initial total number of particles.

For any choice of the initial configuration  $\eta(0)$  in  $\Omega$ , the process will eventually reach the *empty configuration*  $\underline{0}$  corresponding to zero particles in the room which is an absorbing point of the chain.

As alternative working scenario, we will study the dynamics described above also in the presence of a solid obstacle hindering the pedestrian flow in the room. The *obstacle* is made of an array of sites permanently occupied by fictitious particles. In such a way these sites are never accessible to the actual interacting particles within our system.

The dynamics in both the presence and in the absence of the obstacle is the same and all the parameters have the same meaning and take similar values. In other words, we are implicitly assuming that

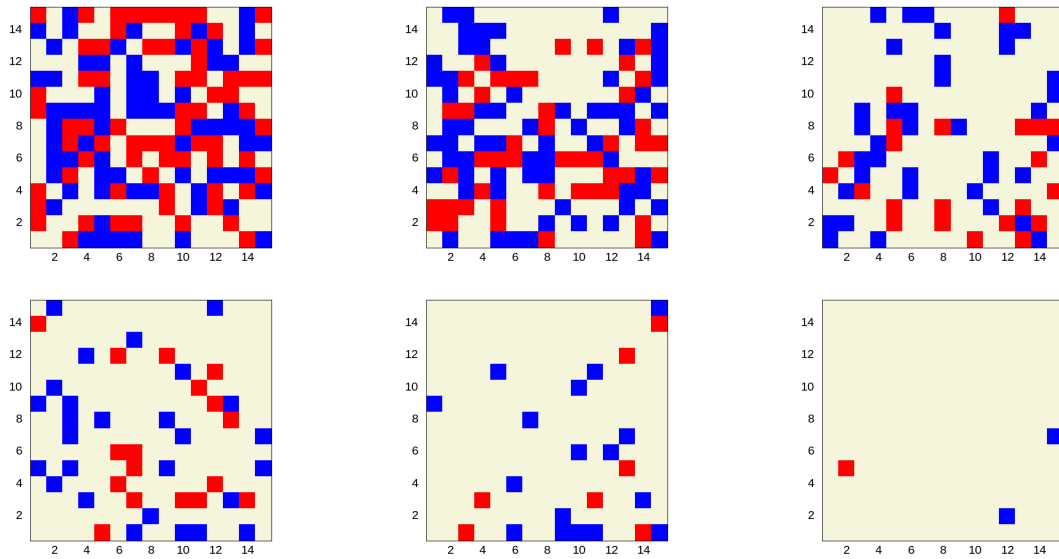


**Figure 2.** Configurations of the model sampled at different times (increasing in lexicographic order). Parameters:  $L = 15$ ,  $w_{\text{ex}} = 7$ ,  $L_v = 5$ , and  $\varepsilon = 0.3$ . Red pixels represent active particles, blue pixels denote passive particles, and gray sites are empty. In the initial configuration (top left panel) there are 70 active and 70 passive particles.

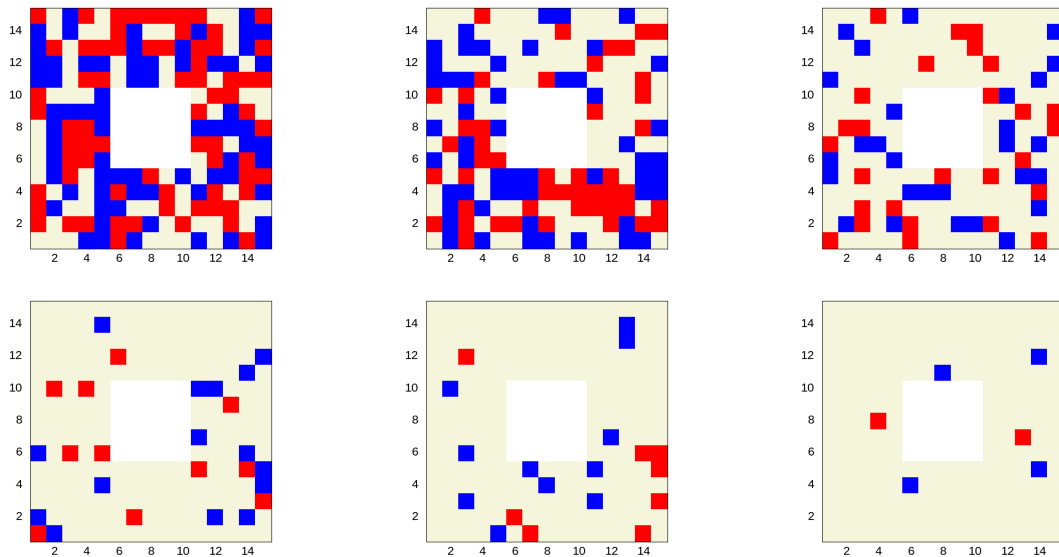


**Figure 3.** As in Figure 2, the obstacle is a centered  $5 \times 5$  square. This fixed obstacle is depicted with white pixels.

the presence of the obstacle does not affect the pedestrian behavior: the obstacle is simply a barrier that must be avoided by the walking pedestrian.

Although, in principle, there is no restriction on the choice of the obstacle geometry, in this framework we always consider centered squared obstacles. A thorough investigation of the effect of the choice of obstacle geometry on the evacuation time for mixed pedestrian populations moving through partially obscure rooms deserves special attention and will be done in a forthcoming work.

We simulate this process using the following scheme: at time  $t$  we extract an exponential random time  $\tau$  with parameter the total rate  $\sum_{\zeta \in \Omega} c(\eta(t), \zeta)$  and set the time equal to  $t + \tau$ . We then select a configuration using the probability distribution  $c(\eta(t), \eta) / \sum_{\zeta \in \Omega} c(\eta(t), \zeta)$  and set  $\eta(t + \tau) = \eta$ .

As we have already pointed out in Section 1, the main goal of the paper is to detect drafting in pedestrian flows, namely, identify situations when the evacuation of passive particles is favored by the presence of the active ones, even if no leadership or other kind of information exchange is allowed. We expect that this phenomenon will be effective, provided the active particles will spend a sufficiently long time in the room. This seems to help efficiently passive particles to escape. This effect is illustrated in the Figures 2 and 3, where we show the configuration of the system at different times both in the absence, and respectively, in the presence of an obstacle. Indeed, the sequences of configurations show that, though the evacuation of active particles is faster than that of the passive ones, even at late times the fraction of active particles is still reasonably high.

### 3. The evacuation time

Consider the dynamics defined in Section 2, given a configuration  $\eta \in \Omega$ . We let  $\tau_\eta$  be the first hitting time to the empty configuration, i.e.

$$\tau_\eta = \inf\{t > 0 : \eta(t) = \mathbf{0}\}, \quad (3.1)$$

for the chain started at  $\eta$ . Given a configuration  $\eta \in \Omega$ , we define the *evacuation time* starting from  $\eta$  as

$$T_\eta = \mathbb{E}_\eta[\tau_\eta]. \quad (3.2)$$

We have defined the evacuation time as the time needed to evacuate all the particles initially in the system, that is to say the evacuation time is the time at which the last particle leaves the room. In this section as well as in the next one, we study numerically the evacuation time for a fixed initial random condition and then produce various realizations of the process for specific values of the initial drift  $\varepsilon$  and of the visibility depth  $L_v$ . To this end, we consider two geometrically different situations: (i) the empty room and (ii) the room with a squared obstacle positioned at the center.

#### 3.1. The empty room case

We consider the system defined in Section 2 for  $L = 15$  (side length of the room),  $w_{\text{ex}} = 7$  (exit width),  $N_p = 70$  (initial number of passive particles)  $N_A = 0, 70$  (initial number of active particles)  $L_v = 2, 5, 7, 15$  (visibility depth), and  $\varepsilon = 0.1, 0.3, 0.5$  (drift). More details are provided in the figure captions.

All the simulations are done starting the system from the same initial configuration chosen once for all by distributing the particle at random with uniform probability. More precisely, two initial

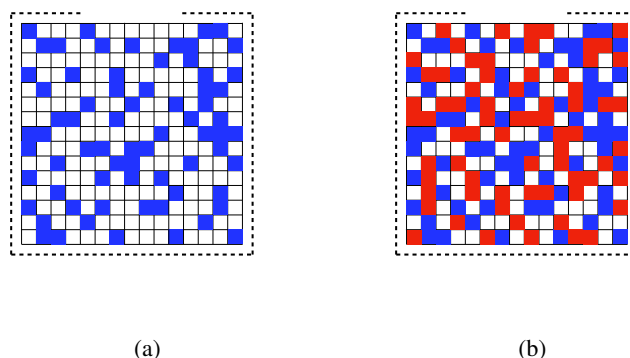


**Figure 4.** Two initial configurations for the lattice gas dynamics. Blue and red pixels represent, respectively, passive and active particles. The thick dashed line surrounding a large fraction of the grid denotes the presence of reflecting boundary conditions. The exit door is located in presence of the missing segment of dashed line. In (a) only  $N_P$  passive particles are present. In (b), the passive particles occupy the same initial positions as in (a), and  $N_A$  active particles are also included (we fix  $N_A = N_P$ ). We shall compare the evacuation time relative to the two configurations in (a) and (b).

configurations are considered, one for the case  $N_P = 70$  and  $N_A = 0$  and one for the case  $N_P = 70$  and  $N_A = 70$ , chosen in such a way that in the two cases the initial positions of the passive particles is the same, see Figure 4 for a schematic illustration.

We then compute the time needed to evacuate all the particles initially in the systems and, by averaging over  $10^5$  different realizations of the process, we compute a numerical estimate of the evacuation time (3.2) for the chosen initial condition. Results are reported in Figure 5.

The main result of our investigation is the following: the evacuation time  $T_\eta$  corresponding to the initial configuration with active particles (see the illustration (b) in Figure 4) is *less* than that corresponding to the initial configuration with sole passive particles (see the illustration (a) in Figure 4). This result is non-trivial since our lattice dynamics is based on a hard core exclusion principle [20] – the motion of particles towards the exit is hindered by the presence of nearby particles. In the context of this work, we refer to this phenomenon as drafting, marking this way the analogy with the drafting or aerodynamic drag effect encountered by pelotons of cyclists racing towards the goal; we refer the reader, for instance, to [21, 22] and references cited therein, for wind tunnel and computational evidence on drafting. It is crucial to note that the presence of active particles is essential for the onset of this phenomenon: if all active particles in the configuration (b) in Figure 4 (represented by the red pixels) were replaced by passive ones (blue pixels), the evacuation time would clearly become larger than with the configuration (a). This is essentially due to the exclusion constraint of the lattice gas dynamics.

In the left panel in Figure 5, the dependence of the evacuation time on the drift  $\varepsilon$  is shown. Open symbols refer to the evacuation time for  $N_P = 70$  and  $N_A = 70$ ; for each value of  $\varepsilon$  we repeat the measure of the evacuation time also for a system in which only passive particles are present. We then obtain the sequence of solid disks reported in the figure which is approximately constant, since the

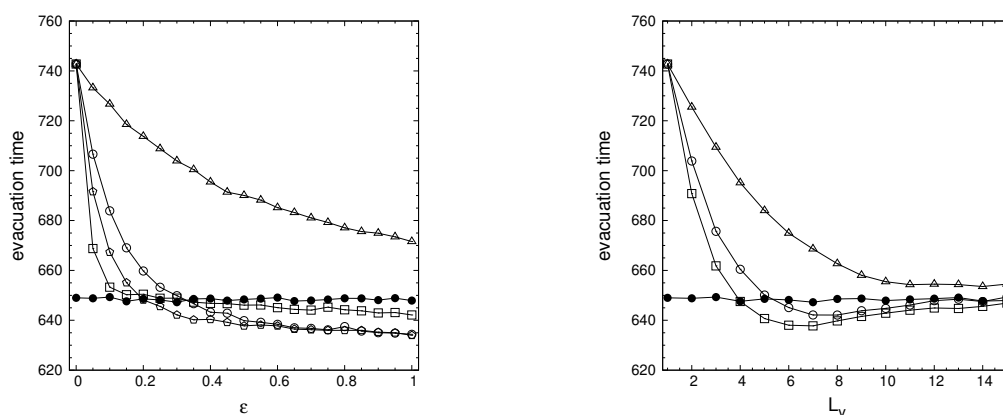


**Figure 5.** Evacuation time in an empty room for  $L = 15$ ,  $w_{\text{ex}} = 7$ ,  $N_A = 0$  and  $N_P = 70$  (solid disks) and  $N_A = N_P = 70$  (open symbols). Left panel:  $L_v = 2$  (open triangles),  $L_v = 5$  (open circles),  $L_v = 7$  (open pentagons),  $L_v = 15$  (open squares). Right panel:  $\varepsilon = 0.1$  (open triangles),  $\varepsilon = 0.3$  (open circles),  $\varepsilon = 0.5$  (open squares).

dynamics of the passive particles does not depend on  $\varepsilon$ . We observe that the small fluctuations visible in the data represented by solid disks Figure 5 come from considering averages over a finite number of different realizations of the process (all starting from the given initial configuration).

Since the number particles in the initial configuration in the experiments with the presence of active particles is double with respect to that considered in the case of only passive particles, one would expect a larger evacuation time. This is indeed the case for a small visibility depth, i.e. for  $L_v = 2$ . In such a case, it is worth noting that the evacuation time decreases when the drift is increased as it is in fact reasonable since a larger drift favors the fast evacuation of active particles, but it remains larger than the evacuation time in absence of active particles for all the values of  $\varepsilon$  that we considered. On the other hand, for larger values of the visibility depth, as long as the drift is large enough, the evacuation time in the presence of active particles becomes smaller than the one measured in the presence of only passive particles.

This effect is rather surprising. It can be interpreted by saying that the presence of active particles, which have some information about the location of the exit, helps passive particles to evacuate the room even if no information exchange is allowed, and, mostly, even in presence of the exclusion constraint of the lattice gas dynamics. Indeed, passive particles continue their blind symmetric dynamics, nevertheless their evacuation time is reduced. The sole interaction among passive and active particles is the exclusion rules, hence one possible interpretation of this effect is that active particles, while walking toward the exit, leave behind a sort of empty sites wake. Passive particles, on the other hand, can benefit of such an empty path and be thus blindly driven towards the exit. A different interpretation is that passive particles, due to the exclusion rule, are pushed by active particles towards the exit.

In the right panel of Figure 5, for the same choices of parameters and initial conditions, we show the evacuation time as a function of the visibility depth  $L_v$  for several values of the drift  $\varepsilon$ . Data can be discussed similarly as we did for those plotted in the left panel of the same figure: for small drift, and for any choice of the visibility length, the evacuation time in presence of active particles is larger than the one measured with sole passive particles. But, if the drift is increased, for a sufficiently large visibility depth, the evacuation time in presence of active particles becomes smaller than the one for

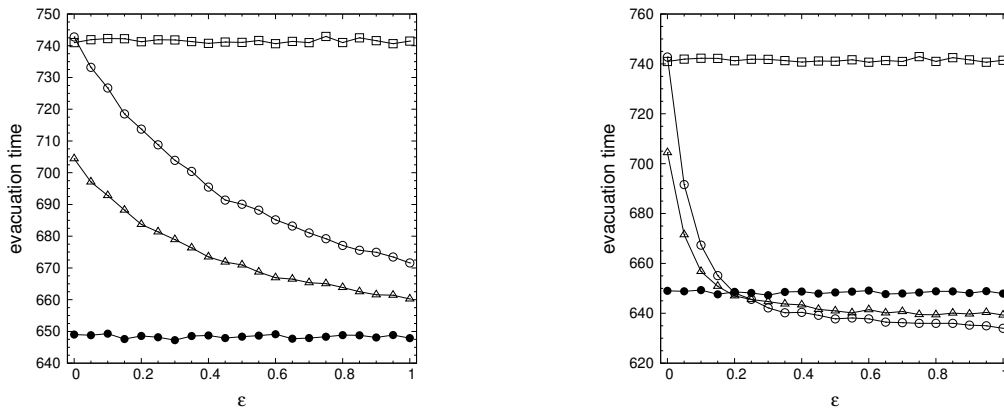


**Figure 6.** Evacuation time in an empty room for  $L = 15$ ,  $w_{\text{ex}} = 7$ ,  $N_A = 0$  and  $N_P = 70$  (solid disks),  $N_A = 35$  and  $N_P = 70$  (open triangles),  $N_A = 70$  and  $N_P = 70$  (open circles) and  $N_A = 0$  and  $N_P = 140$  (open squares). Left panel:  $L_v = 2$ . Right panel:  $L_v = 7$ .

sole passive particles though the total number of particles to be evacuated is doubled. As before we interpret these data as an evidence of the presence of the drafting effect.

Remarkably, for sufficiently large drift  $\varepsilon$ , the evacuation time is not monotonic with respect to the visibility depth. In other words, there is an optimal value of  $L_v$  which minimizes the evacuation time. The fact that for  $L_v$  too large, i.e., comparable with the side length of the room, the evacuation time increases with  $L_v$  can be explained remarking that if active particles exit the system too quickly then passive particles, left alone in the room, evacuate it with their standard time. Hence, the drafting effect is visible as long as the parameters  $\varepsilon$  and  $L_v$  make the motion of the active particles towards the exit enough faster than that of passive particles, but not too fast. Indeed, if the active particles move too slowly, they behave as passive ones: this would make the evacuation time larger, due to the standard exclusion constraint of our lattice gas dynamics. On the other hand, if the active particles move too fast, passive particles remain soon alone on the lattice, therefore the evacuation time relative to the configuration of type (b) in Figure 4 reduces to that relative to the configuration of type (a).

Before concluding this Section, we shall also highlight the effect of varying the relative amount of active and passive particles in the initial configuration. In Figure 6 we also present the average evacuation times for the cases with  $N_P = 70$ ,  $N_A = 35$  and  $N_P = 140$ ,  $N_A = 0$ , for two different values of  $L_v$ . One readily notices that when the number of passive particles is doubled (case  $N_P = 140$  and  $N_A = 0$ ) the evacuation time increases and it obviously results to be independent of  $\varepsilon$  and  $L_v$ . For small visibility depth ( $L_v = 2$  in the left panel in Figure 6) the evacuation time for the case  $N_A = 35$  and  $N_P = 70$  is smaller than the one measured in the case  $N_A = 70$  and  $N_P = 70$  for any  $\varepsilon$  and shows a monotonic decrease. The results are more interesting for larger visibility depth ( $L_v = 7$  in the right panel in Figure 6): if the drift  $\varepsilon$  is large enough, namely, larger than about 0.2, the total evacuation time in presence of active particles becomes smaller than the one measured for sole passive particles both for the case  $N_A = 35$  and  $N_P = 70$  and  $N_A = 70$  and  $N_P = 70$ , that is to say, in both cases the drafting effect shows up. More interestingly, the evacuation time is smaller in the case in which more active particles are present (open circles in the picture): this is a sort of signature of the drafting effect.

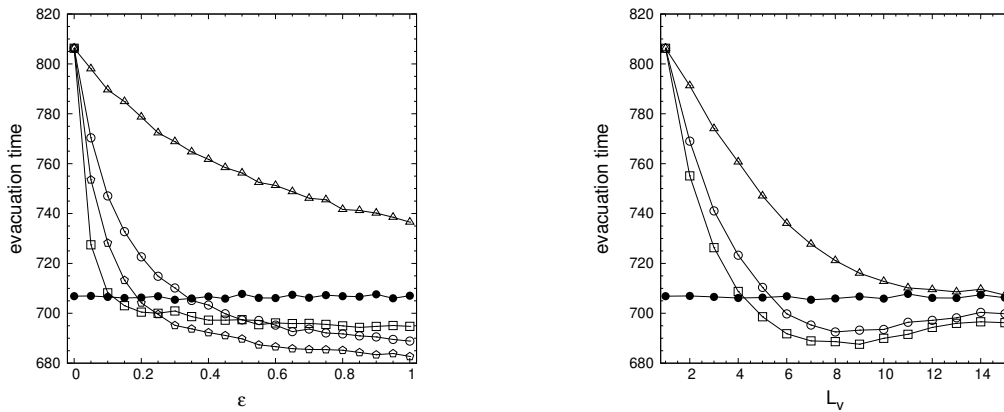


**Figure 7.** Evacuation time in a room with a  $5 \times 5$  squared centered obstacle for  $L = 15$ ,  $w_{\text{ex}} = 7$ ,  $N_A = 0$  and  $N_P = 70$  (solid disks) and  $N_A = N_P = 70$  (open symbols). Left panel:  $L_v = 2$  (open triangles),  $L_v = 5$  (open circles),  $L_v = 7$  (open pentagons),  $L_v = 15$  (open squares). Right panel:  $\varepsilon = 0.1$  (open triangles),  $\varepsilon = 0.3$  (open circles),  $\varepsilon = 0.5$  (open squares).

### 3.2. The room with an obstacle

Simulations similar with those described in Section 3.1 have been run in presence of a centered square obstacle made of  $5 \times 5$  sites of the room not accessible by both active and passive particles. As before, we have computed the evacuation time in such a case and results are reported in Figure 7.

It is immediate to remark that plots in Figure 7 are very similar to those shown in Figure 5. Our interpretation of the results is then the same. We just mention that the vertical scale is slightly different and we notice that, in presence of an obstacle, the drafting effect is slightly increased. The fact that the presence of an obstacle with suitable geometry can favor the evacuation of a room is a fact already established in the literature, see, e.g., [6, 14–16] and references therein.

## 4. The stationary flux

To detect non-trivial behaviors as time elapses beyond a characteristic walking timescale, we consider now a modified version of the model proposed in Section 2. Essentially, the current situation is as follows: Particles exiting the system are introduced back in one site, randomly chosen among the empty sites of the room so that the total number of active and passive particles is approximately kept constant during the evolution. This way, the system reaches a final stationary state and in such a state we shall measure the flux of exiting active and passive particles.

The main idea is to add a *reservoir* in which particles exiting the room are collected. Particles in the reservoir are then introduced inside  $\Lambda$  with rates depending on the number of particles in such a reservoir and on the number of empty sites in the room.

More precisely, recall the definition of the number of active and passive particles  $n_A(\eta)$  and  $n_P(\eta)$  in the configuration  $\eta$  and fix two non-negative integer numbers  $N_A$  and  $N_P$ . Consider the Markov process defined in Section 2 with an initial configuration with total number of active and passive particles respectively equal to  $N_A$  and  $N_P$  and rates  $c(\eta, \eta')$ , for  $\eta, \eta' \in \Omega$ , defined as in Section 2 with the

following modification:

- if  $\eta'$  can be obtained by  $\eta$  by adding a +1 at an empty site  $x$  then  $c(\eta, \eta') = [N_A - n_A(\eta)] / (L^2 - n_A(\eta) - n_P(\eta))$  (moving an active particle from the reservoir to an empty site in the room);
- if  $\eta'$  can be obtained by  $\eta$  by adding a -1 at an empty site  $x$  then  $c(\eta, \eta') = [N_P - n_P(\eta)] / (L^2 - n_A(\eta) - n_P(\eta))$  (moving a passive particle from the reservoir to an empty site in the room).

At time  $t$ , the quantities  $N_A - n_A(\eta(t))$  and  $N_P - n_P(\eta(t))$  represent the number of active, and respectively, passive particles in the reservoir at time  $t$ , whereas  $L^2 - n_A(\eta(t)) - n_P(\eta(t))$  is the number of empty sites of the room at time  $t$ .

With these changes in the definition of the rate, the total number of particles in the system (considering the room and the reservoir) is conserved. The number of particles in the room, on the other hand, will fluctuate due to the fact that particles can accumulate in the reservoir.

In the study of this dynamics, the main quantity of interest is the stationary *outgoing flux* or *current* which is the value approached in the infinite time limit by the ratio between the total number of particle that in the interval  $(0, t)$  jumped from the exit to the reservoir and the time  $t$ .

#### 4.1. The empty room case

We consider the system defined in Section 4 for  $L = 15$  (side length of the room),  $w_{\text{ex}} = 7$  (exit width),  $N_P = 70$  (number of passive particles)  $N_A = 0, 70$  (number of active particles)  $L_v = 2, 5, 7, 15$  (visibility depth), and  $\varepsilon = 0.1, 0.3, 0.5$  (drift). More details on the selected parameters regimes are provided in the figure captions.

As in Section 3.1, all the simulations share the same initial configuration obtained by distributing the particle at random with a uniform probability. More precisely, two initial configurations are considered, one for the case  $N_P = 70$  and  $N_A = 0$  and one for the case  $N_P = 70$  and  $N_A = 70$ , chosen in such a way that in the two cases the initial positions of the passive particle is the same, see Figure 4.

We then let the system evolve and compute the ratio of the number of particles jumping from the exit to the reservoir to time. We consider, in particular, the flux of passive particles, in *absence* and in *presence* of the active ones. This observable fluctuates until it approaches a roughly constant value after about  $k = 6.36 \times 10^7$  MC steps (corresponding, approximately, to time 328342) is reached. Our results are reported in Figure 8.

We show the dependence of the stationary flux of passive particles on the drift  $\varepsilon$  in the left panel of Figure 8. Open symbols refer to the flux for  $N_P = 70$  and  $N_A = 70$ ; for each value of  $\varepsilon$  we repeat the measure of the flux time also for a system in which only passive particles are present. We then obtain the sequence of solid disks reported in the figure which is approximatively constant, since the dynamics of the passive particles does not depend on  $\varepsilon$ .

In the right panel of Figure 8, for the same choices of parameters and initial conditions, we show the stationary flux as a function of the visibility depth  $L_v$  for several values of the drift  $\varepsilon$ .

Both figures exhibit firstly an increase of the flux in presence of active particles at zero drift or zero visibility depth with respect to the case in which only passive particles are present (filled disks in Figure 8). This situation can be understood by considering that, despite the exclusion constraint of the lattice gas dynamics, doubling the number of particles can justify the increase of the flux at zero drift, if no complete clogging is reached. It is instructive to follow the sequence of empty symbols in Figure 8 for increasing values of  $\varepsilon$  or  $L_v$ . Note that an increase of the drift yields a monotonic increase

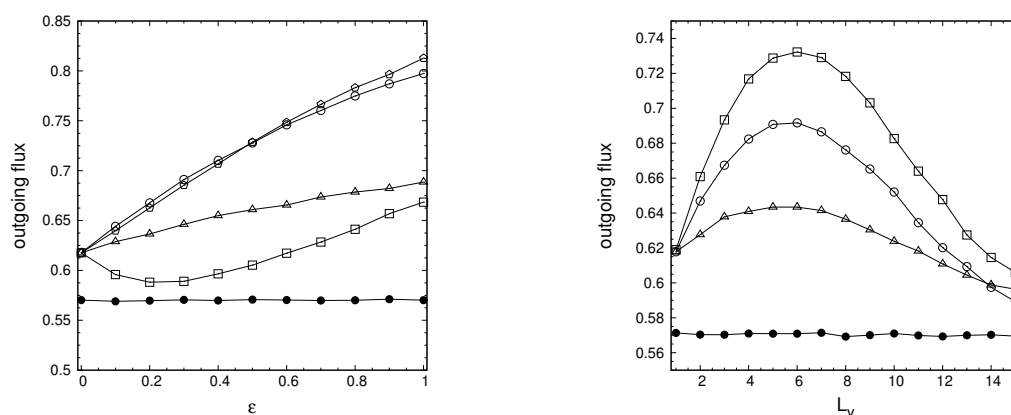


**Figure 8.** Stationary flux of passive particles in an empty room for  $L = 15$ ,  $w_{\text{ex}} = 7$ ,  $N_A = 0$  and  $N_P = 70$  (solid disks) and  $N_A = N_P = 70$  (open symbols). Left panel:  $L_v = 2$  (open triangles),  $L_v = 5$  (open circles),  $L_v = 7$  (open pentagons),  $L_v = 15$  (open squares). Right panel:  $\varepsilon = 0.1$  (open triangles),  $\varepsilon = 0.3$  (open circles),  $\varepsilon = 0.5$  (open squares).

of the stationary flux as long as the visibility depth is not too large. In fact, the monotonic increase of the flux is not observed with  $L_v = 15$  (see the open squares in the left panel). This means that in the presence of such a large visibility depth the evacuation of the passive particles can be hindered by the presence of active particles if the drift is not large enough.

A quite interesting and a priori unexpected fact is the non-monotonicity of the stationary flux with respect to the visibility depth: this can be seen by looking at the different curves in the left panel and it is also put in evidence in the plots of the right panel.

It is also worth looking at the behavior of the transient fluxes as functions of time in the same evacuation set-up discussed earlier in Section 3, in which no external particle reservoir is included. To this aim, for a given initial condition, we averaged the flux of passive particles over  $10^3$  different realizations of the process. Coherently with the behavior observed for the stationary fluxes in Figure 8, we notice once more that the presence of active particle enhances the outgoing flux of passive particles, for all the considered values of  $\varepsilon$  and  $L_v$ , this being again a trace of the underlying drafting phenomenon.

To get a deeper insight in this interesting effect, we show in Figure 10 the stationary occupation number profile. To obtain these results, we have run the dynamics for a sufficiently long time (order of  $6.36 \times 10^7$  MC steps) so that the system reaches the stationary state. Starting off from that time, we have averaged the occupation number  $|\eta_x(t)|$  over time at each site of the room. The resulting function takes values between zero and one; see Figure 10 for an illustration.

The plots indicate that for large drift and large visibility depth that clogging along the median vertical line can take place. the occurrence of such clogging situations partly explain the not-monotonic behavior of the stationary flux with varying the visibility depth.

The emergence of the central clogging is related to the large value of the drift pointing towards the central direction. This phenomenon reminds the faster-is-slower behavior already pointed out in the literature [23, 24], even if in this case the origin of the phenomenon can be traced back to the intensity of the drift rather than to the pedestrian speed.

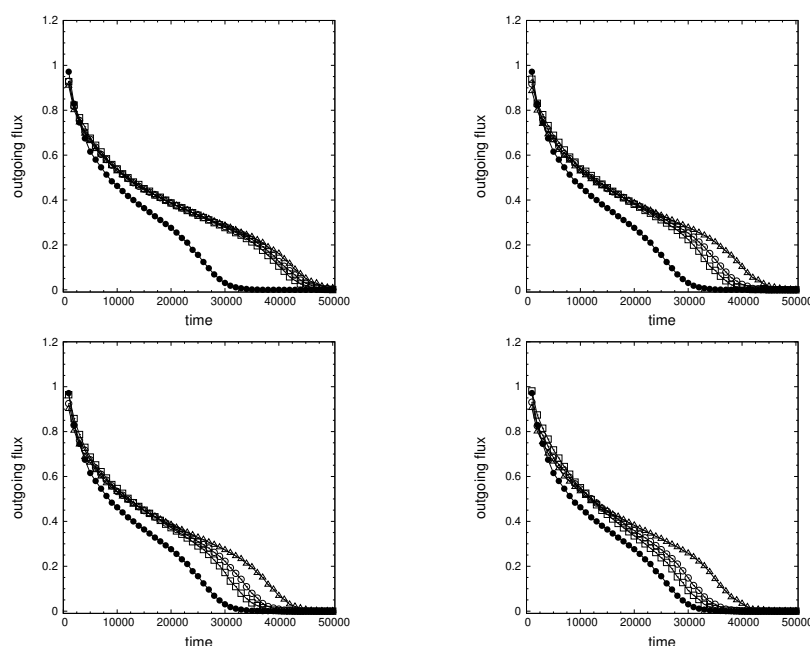


**Figure 9.** Transient flux of passive particles in an empty room for  $L = 15$ ,  $w_{\text{ex}} = 7$ ,  $N_A = 0$  and  $N_P = 70$  (solid disks) and  $N_A = N_P = 70$  (open symbols). In the various panels, shown are the cases with  $\varepsilon = 0.1$  (empty triangles),  $\varepsilon = 0.3$  (empty circles) and  $\varepsilon = 0.5$  (empty squares). Different values of  $L_v$  are considered:  $L_v = 2$  (top left panel),  $L_v = 5$  (top right panel),  $L_v = 7$  (bottom left panel), and  $L_v = 15$  (bottom right panel).

#### 4.2. The room with an obstacle

Simulations similar with those described in Section 4.1 have been run in presence of a centered square obstacle made of  $5 \times 5$  sites of the room not accessible by both active and passive particles. As before, we have computed the stationary flux and our results are reported in Figure 11.

The results plotted in Figures 11 and 12 are very similar to those shown in Figure 8 and 10. Our interpretation of the results is essentially the same. Mind though that, in order to reach the stationary state, we had to run the dynamics for a larger time than in the case of the empty room model (i.e., of order of  $9.0 \times 10^7$  MC steps). Also from the point of view of the computed stationary flux measures, our results suggest that the presence of the obstacle slightly favors the exit of particles from the room. This was noted in Section 3.2 in connection with the evacuation time measurements; see also [6, 14–16].

Comparing Figures 8 and 11 one realizes that the dependence of the stationary flux on the drift and on the visibility depth is milder. This fact can be explained remarking that the phenomenon of accumulation of particles along the median vertical line of the room discussed in Section 4.1 is less evident. Again, the obstacle seems to be keeping particles far apart so that clogging is reduced.

## 5. Conclusions

We studied the problem of the evacuation of a crowd of pedestrians from an obscure region. We start from the assumption that the crowd is made of both active and passive pedestrians. The hazardous motion of pedestrians due to lack of light and, possibly, combined also to a high level of stress is

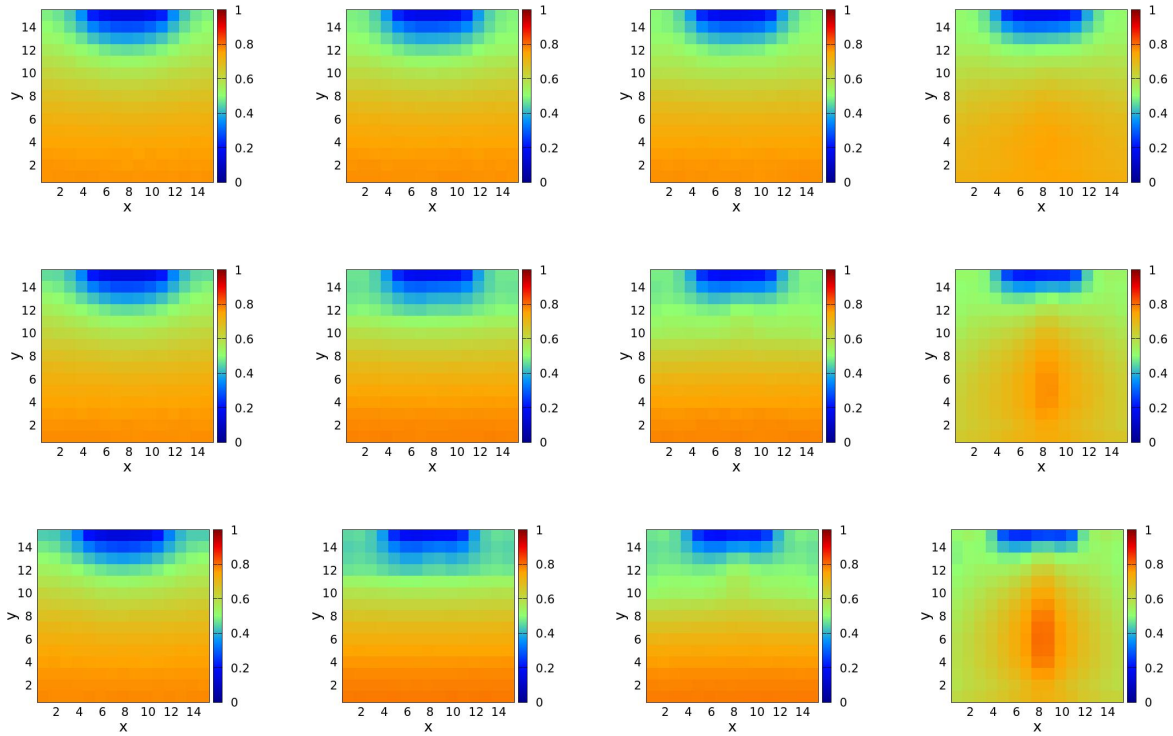


**Figure 10.** Occupation number profile at stationarity for  $L = 15$ ,  $w_{\text{ex}} = 7$ ,  $x_{\text{ex}} = 5$ ,  $N_A = N_P = 70$ ,  $\varepsilon = 0.1, 0.3, 0.5$  (from the top to the bottom),  $L_v = 2, 5, 7, 15$  (from the left to the right).

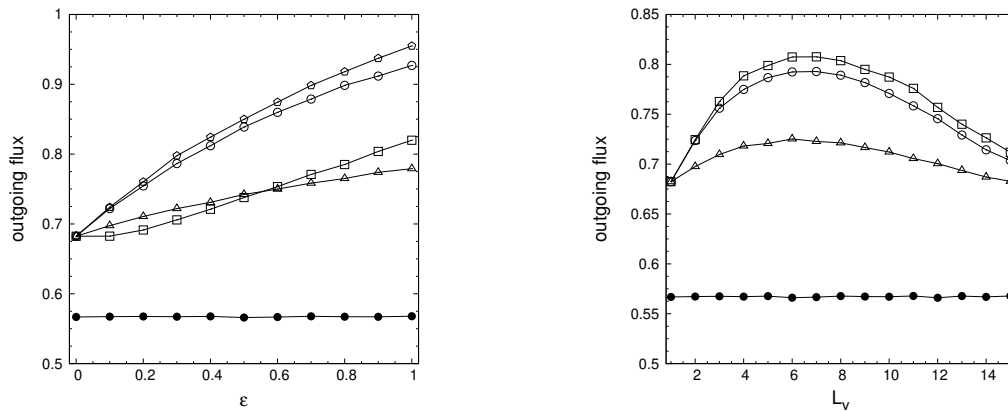


**Figure 11.** Stationary flux in a room with a  $5 \times 5$  squared centered obstacle for  $L = 15$ ,  $w_{\text{ex}} = 7$ ,  $N_A = 0$  and  $N_P = 70$  (solid disks) and  $N_A = N_P = 70$  (open symbols). Left panel:  $L_v = 2$  (open triangles),  $L_v = 5$  (open circles),  $L_v = 7$  (open pentagons),  $L_v = 15$  (open squares). Right panel:  $\varepsilon = 0.1$  (open triangles),  $\varepsilon = 0.3$  (open circles),  $\varepsilon = 0.5$  (open squares).

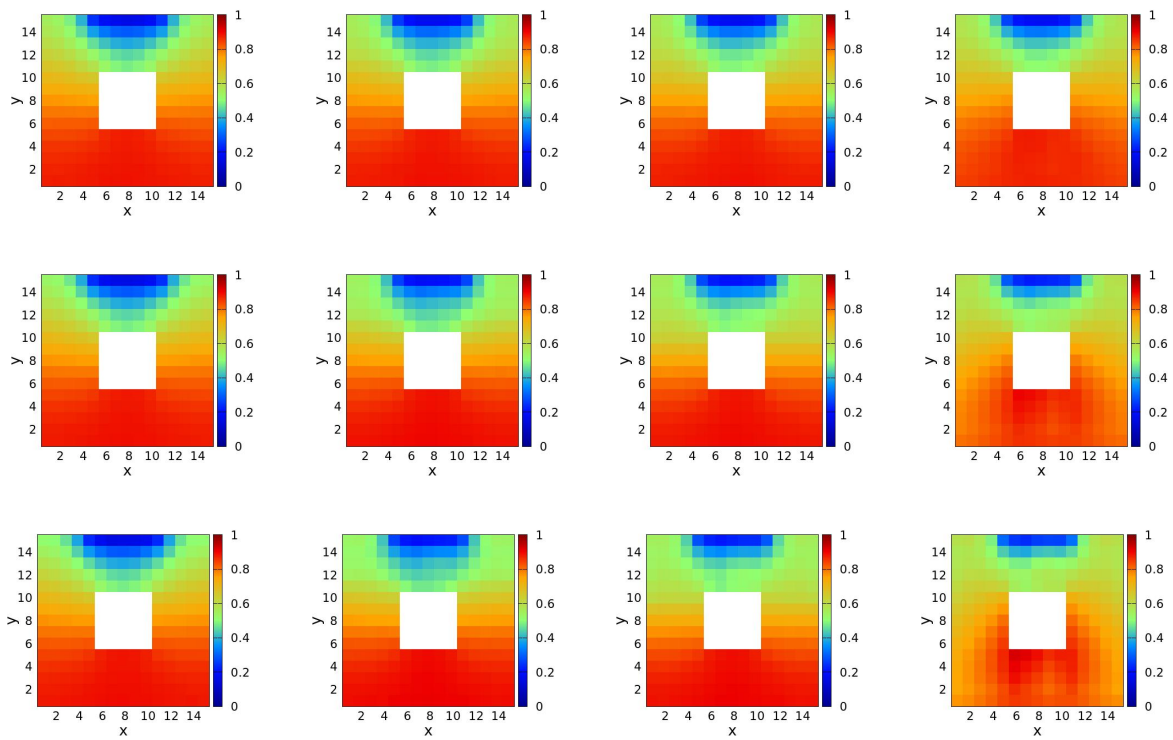


**Figure 12.** Occupation number profile at stationarity in presence of a  $5 \times 5$  centered obstacle for  $L = 15$ ,  $w_{\text{ex}} = 7$ ,  $x_{\text{ex}} = 5$ ,  $N_A = N_P = 70$ ,  $\varepsilon = 0.1, 0.3, 0.5$  (from the top to the bottom),  $L_v = 2, 5, 7, 15$  (from the left to the right).

modeled via a simple random walk with exclusion. The active (smart, informed, aware, ...) pedestrians, which are aware of the location of the exit, are supposed to be subject to a given drift towards the exit, while the passive (unaware, uninformed) pedestrians are performing a random walk within the walking geometry and eventually evacuate if they accidentally find the exit. The particle system is strongly interacting via the site exclusion principle – each site can be occupied by only a single particle.

The main observable is the evacuation time as a function of the parameters characterizing the motion of the aware pedestrians. We have found that the presence of the active pedestrians favors the evacuation of the passive ones. This is rather surprising since we explicitly do not allow for any communication among the pedestrians. This seems to be due to some sort of drafting effect. A drag seems to arise due to the empty spaces left behind by the active pedestrians moving towards the exit and naturally filled by the completely random moving unaware pedestrians.

We have also remarked that too smart active pedestrians can limit the drafting effect: indeed, if they exit the room too quickly the unaware pedestrian do not have the time to take profit of the wakes of empty side that they left during their motion towards the exit.

A promising research line concerns the investigation of evacuation times when different species of particles are assumed to choose among different exit doors. Such topic is relevant not only for urban situations but also for tunnel fires or for forest fires expanding towards the neighborhood of inhabited regions.

The main open question in this context is the model validation. A suitable experiment design is needed to make any progress in this sense. This will be our target in forthcoming work.

With regards to the building up of the aerodynamic drag, it would also be interesting to verify the onset of the drafting phenomenon in lattice gas models in the presence of non-standard transport regimes leading to uphill diffusion of particles; see [25] (and references cited therein) for the study of such transport mechanisms.

## Acknowledgments

ENMC and MC thank FFABR 2017 for financial support. We thank our collaborators Omar Richardson (Karlstad, Sweden) and Errico Presutti (Gran Sasso Science Institute, Italy) for very useful discussions on this and related topics, and Finn Nilson (Karlstad) for providing us with infos about the 2001 Roskilde Festival incident and the 1989 Hillsborough Disaster, mentioned in the footnote of p. 2.

## Conflict of interest

There is no conflicts of interest.

## References

1. G. Albi, M. Bongini, E. Cristiani, et al., Invisible control of self-organizing agents leaving unknown environments, *SIAM J. Appl. Math.*, **76** (2016), 1683–1710.
2. K. Fridolf, E. Ronchi, D. Nilsson, et al., Movement speed and exit choice in smoke-filled rail tunnels, *Fire Safety J.*, **59** (2013), 8–21.

3. F. Müller, O. Wohak and A. Schadschneider, Study of influence of groups on evacuation dynamics using a cellular automaton model, *Transport. Res. Procedia*, **2** (2014), 168–176.
4. J.–H. Wang and J.–H. Sun. Principal aspects regarding to the emergency evacuation of large-scale crowds: A brief review of literatures until 2010, *Procedia Eng.*, **71** (2014), 1–6.
5. S. Xue, B. Jia, R. Jiang, et al., Pedestrian evacuation in view and hearing limited condition: The impact of communication and memory, *Phys. Lett. A*, **380** (2016), 3029–3035.
6. A. Ciallella, E. N. M. Cirillo, P. Curseu, et al., Free to move or trapped in your group: Mathematical modeling of information overload and coordination in crowded populations, *Math. Mod. Meth. Appl. Sci.*, **28** (2018), 1831–1856.
7. C. von Krüchten and A. Schadschneider, Empirical study on social groups in pedestrian evacuation dynamics, *Physica A*, **475** (2017), 129–141.
8. H. Oh and J. Park, Main factor causing “faster-is-slower” phenomenon during evacuation: rodent experiment and simulation, *Sci. Rep.*, **7** (2017), 13724.
9. M. Colangeli, A. Muntean, O. Richardson, et al., Modelling interactions between active and passive agents moving through heterogeneous environments, in G. Libelli, N. Bellomo (Eds), *Crowd Dynamics*, vol. 1: Theory, Models and Safety Problems (pp. 211–254). Modeling and Simulation in Science, Engineering and Technology, Boston, Birkhäuser, 2019.
10. O. Richardson, A. Jalba and A. Muntean, The effect of environment knowledge in evacuation scenarios involving fire and smoke – a multiscale modelling and simulation approach, *Fire Technol.*, **55** (2019), 415–436.
11. J. P. Agnelli, F. Colasuonno and D. Knopoff, A kinetic theory approach to the dynamics of crowd evacuation from bounded domains, *Math. Mod. Meth. Appl. S.*, **25** (2015), 109–129.
12. N. Bellomo, D. Clarke, L. Gibelli, et al., Human behaviours in evacuation crowd dynamics: From modelling to “big data” toward crisis management, *Phys. Life Rev.*, **18** (2016), 1–21.
13. E. Cristiani, B. Piccoli and A. Tosin, *Multiscale Modeling of Pedestrian Dynamics*, Series in Modeling, Simulation and Applications, vol. 12, Springer, 2014.
14. A. Ciallella and E. N. M. Cirillo, Linear Boltzmann dynamics in a strip with large reflective obstacles: stationary state and residence time, *Kinetic Relat. Mod.*, **11** (2018), 1475–1501.
15. E. N. M. Cirillo, O. Krehel, A. Muntean, et al., Lattice model of reduced jamming by a barrier, *Phys. Rev. E*, **94** (2016), 042115.
16. E. Cristiani and D. Peri. Handling obstacles in pedestrian simulations: Models and optimization, *Appl. Math. Model.*, **45** (2017), 285–302.
17. I. D. Couzin, J. Krause, N. R. Franks, et al., Effective leadership and decision-making in animal groups on the move. *Nature*, **433** (2005), 513–516.
18. D. Andreucci, D. Bellaveglia, E. N. M. Cirillo, et al., Monte Carlo study of gating and selection in potassium channels. *Phys. Rev. E*, **84** (2011), 021920.
19. G. A. Pavliotis, *Stochastic Processes and Applications: Diffusion Processes, the Fokker-Planck and Langevin Equations*. Texts in Applied Mathematics, vol. 60, Springer Verlag, Berlin, 2014.

20. H. Spohn, *Large Scale Dynamics of Interacting Particles*, Springer-Verlag Berlin Heidelberg, 1991.
21. B. Blocken, T. van Druenen, Y. Toparlar, et al., Aerodynamic drag in cycling pelotons: new insights by CFD simulation and wind tunnel testing, *J. Wind Eng. Ind. Aerod.*, **179** (2018), 319–337.
22. B. Blocken, Y. Toparlar, T. van Druenen, et al., Aerodynamic drag in cycling team time trials, *J. Wind Eng. Ind. Aerod.*, **182** (2018), 128–145.
23. D. Helbing, I. Farkas and T. Vicsek, Simulating dynamical features of escape panic, *Nature*, **407** (2000), 487–490.
24. A. Kirchner and A. Schadschneider, Simulation of evacuation processes using a bionics–inspired cellular automaton model for pedestrian dynamics, *Physica A*, **312** (2002), 260–276.
25. M. Colangeli, A. De Masi and E. Presutti, Microscopic models for uphill diffusion, *J. Phys. A: Math. Theor.*, **50** (2017), 435002.



AIMS Press

©2020 the Author(s), licensee AIMS Press. This is an open access article distributed under the terms of the Creative Commons Attribution License (<http://creativecommons.org/licenses/by/4.0>)